84

Development of a Domain Decomposition Method for Computational Aeroacoustics

G. S. Djambazov, C.-H. Lai, and K. A. Pericleous

1 Introduction

Computational Aeroacoustics (CAA) implies the direct simulation of acoustic fields generated by flows and of the interaction of acoustic fields with flows. 'Direct' implies that the computation is only based on fundamental physical principles without reliance on empirical results or heuristic conjectures.

Since sound can be represented as comprised of different frequencies it is not difficult to estimate the resolution requirements for a typical domain, say around an airport, and a typical frequency range of interest, say up to about 100 Hz. If the ecologically important zone — immediately after take-off — is assumed to be 300 m long, 300 m wide, and 100 m high, and if 10 is assumed to be a reasonable number of grid points per wavelength, then the total number of grid points in this computational domain will be about 230 million. This shows that for realistic problems the computing power required with a direct approach is exceedingly large.

The classical approach to aerodynamic noise is Lighthill's "Acoustic Analogy" [Lig52] which does not involve direct computation of the sound field. It can be used to estimate the level of noise generated by some turbulent flows, but not the nonlinear interaction between the flow and the sound waves.

Since fluid flow can be easily computed using Computational Fluid Dynamics (CFD) techniques it is desirable to make use of existing CFD codes as much as possible. The region of interest is then most often split in two: 'near field' with nonlinear acoustic effects, and 'far field' of linear acoustics [SHM95, SH93]. CFD is meant to be used in the near field. In fact most CFD codes suffer from false (numerical) diffusion and will tend to lose the noise too near the place it is generated. Hence, they have to be combined with an Acoustic Analogy, which easily handles the far field [SH93, ZRL95].

If there is a code to compute the near field accurately enough, Kirchhoff's surface integral method can be applied to the far field [Lyr93]. Accordingly, any quantity which follows the wave equation outside a given surface is defined by its values, spatial and

Ninth International Conference on Domain Decomposition Methods
Editor Petter E. Bjørstad, Magne S. Espedal and David E. Keyes

temporal derivatives on the same surface. The Kirchhoff surface should be chosen far enough to contain all the nonlinearities of the near field, and still close enough to form a reasonably sized computational domain.

This paper describes the initial stages of the development of a CAA code for the near field. Following the domain decomposition approach certain modules of this code are shown to be useful in the far field as well.

2 Decomposition of the Variables

Sound is a form of fluid motion, and as such it is governed by the equations of continuity (2.1) and momentum (2.2). Any fluid quantity has been represented as a sum of a 'mean' value (indexed with $_0$), and a 'perturbation' value with no index. The index summation convention is in use:

$$\frac{\partial(\rho_0+\rho)}{\partial t}+\frac{\partial}{\partial x_j}\left[(\rho_0+\rho)(v_{j0}+v_j)\right]=0, \tag{2.1}$$

$$(\rho_0+\rho)\left[\frac{\partial(v_{i0}+v_i)}{\partial t}+(v_{j0}+v_j)\frac{\partial(v_{i0}+v_i)}{\partial x_j}\right]+\frac{\partial(p_0+p)}{\partial x_i}=F_{i0}+F_i. \tag{2.2}$$

The symbols ρ, v, p denote respectively the fluid density, velocity and pressure while F contains both external forces and internal friction.

There are good reasons for splitting the variables [VS95]. Physically, sound waves are small perturbations to other large scale motions, such as wind, and numerically they are best represented separately. Also, in this way existing CFD codes can be used to solve the 'mean flow'.

After expanding the brackets many new terms appear in the governing equations, and an analysis has been made for the magnitude of each of these. For a typical aeroacoustic problem, terms containing a perturbation quantity are very small compared to the rest; terms with derivatives of perturbation quantities are not necessarily so. When all the small terms are moved to the right-hand side, equations (2.3) and (2.4) are obtained:

$$\frac{\partial\rho}{\partial t}+v_{j0}\frac{\partial\rho}{\partial x_j}+\rho_0\frac{\partial v_j}{\partial x_j}=\cdots=q, \tag{2.3}$$

$$\rho_0\left(\frac{\partial v_i}{\partial t}+v_{j0}\frac{\partial v_i}{\partial x_j}\right)+\frac{\partial p}{\partial x_i}=F_i-\cdots=f_i. \tag{2.4}$$

These will be the governing equations for the CAA algorithm. With the mean-flow values defined by CFD the left-hand side is linear, and the small right-hand side can be solved for iteratively. Based on the above analysis fast convergence is expected.

The interaction between CFD and CAA is pictured in Figure 1. It is generally assumed that back-reaction of the sound on the flow field is only to be expected when there is a resonator nearby [Lig52], and that is denoted by the dotted arrow. In most cases iterations in that outermost loop will not be necessary.

Figure 1 Interaction between CFD and CAA codes

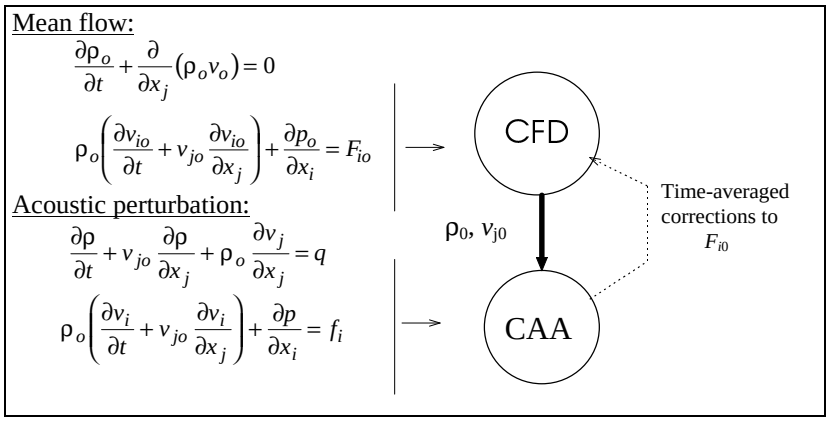

3 Linear Propagation Solver

The discussion above has made it clear that to study the generation of aerodynamic noise one has to resolve also its propagation, which occurs simultaneously. That can be done by a hyperbolic solver, which will become a module in a nonlinear code for the sound-generation zone. It can also be used on its own for the propagation zone, where the linearized Euler equations [SHM95] are most often assumed.

Using the standard definition for the speed of sound, c, the framework for a two-dimensional simulation is presented below:

$$\frac{\partial p}{\partial t} + c\left(\frac{\partial u}{\partial x} + \frac{\partial v}{\partial y}\right) = c^2 q, \tag{3.5}$$

$$\frac{\partial u}{\partial t} + c\frac{\partial p}{\partial x} = cf_x\,,\ u = \rho_0 c v_x, \tag{3.6}$$

$$\frac{\partial v}{\partial t} + c\frac{\partial p}{\partial y} = cf_y\,,\ v = \rho_0 c v_y, \tag{3.7}$$

$$\frac{\partial p}{\partial \rho} = c^2 = \gamma\frac{p_0}{\rho_0}\ (\gamma_{air} = 1.4).$$

Perturbation velocity components along the axes x and y are denoted v_x and v_y, respectively. The right-hand sides are now considered known. At any time step a relative frame of reference — moving with the mean flow — is considered, hence there are no convection terms left.

The finite volume approach has been followed for the discretization of these equations. Successive integration along x, y, and t using the notation of Figure 2

Figure 2 Finite volume formulation – cell-face symbols

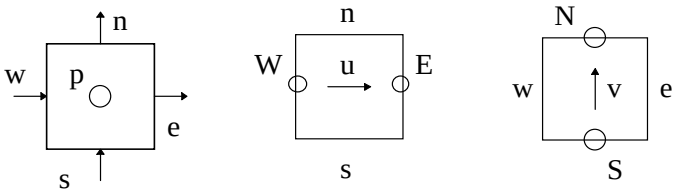

Figure 3 Sample results for the fully explicit numerical scheme
56 time steps, Courant number = 0.7

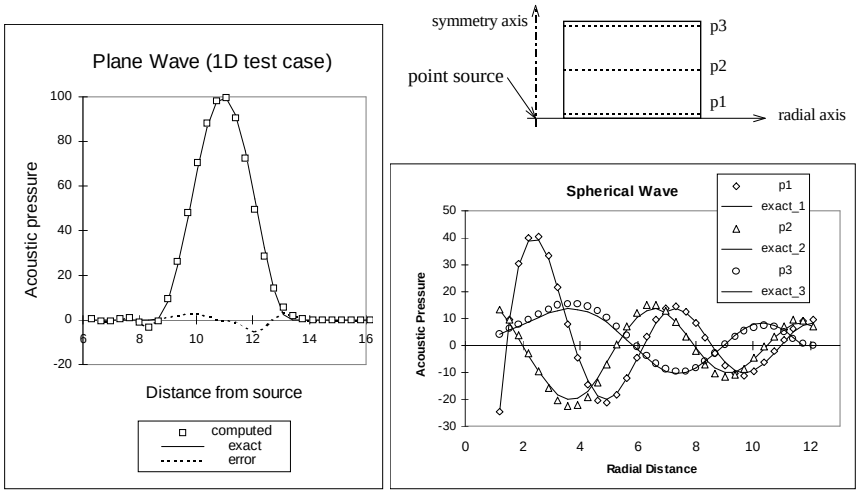

yields:

$$\int_{cell}(p-p_{old})dxdy + c\Delta t\left[\int_{s}^{n}(u_e-u_w)dy + \int_{w}^{e}(v_n-v_s)dx\right] = c^2\Delta t\int_{cell} q\,dxdy,$$

$$\int_{cell}(u-u_{old})dxdy + c\Delta t\int_{s}^{n}(p_E-p_W)dy = c\Delta t\int_{cell} f_x dxdy,$$

$$\int_{cell}(v-v_{old})dxdy + c\Delta t\int_{w}^{e}(p_N-p_S)dx = c\Delta t\int_{cell} f_y dxdy.$$

Integration along the time axis is expressed here through mean values for simplicity.

The Fully Explicit Numerical Scheme

Scalar quantities (i.e., pressure) are stored in the centres of the finite-volume cells while vector quantities (i.e., velocity components) are stored at the cell faces in the middle of the time steps. All integrals are approximated by stepwise functions. The resulting explicit scheme is then the same as the one resulting from a finite-difference approach:

$$\begin{aligned} p &= p_{old} - Cou[(u_e - u_w) + (v_n - v_s)] + c^2 \Delta t q, \\ u &= u_{old} - Cou(p_E - p_W) + c\Delta t f_x, \\ v &= v_{old} - Cou(p_N - p_S) + c\Delta t f_y, \\ Cou &= c\Delta t/h, \end{aligned}$$

where Δt is the length of the time step, and h is the size of the cells on a regular mesh.

This scheme was first tested in one dimension, which is the case of plane wave propagation (with $v = 0$) because exact analytical solutions can be obtained for plane waves (1D) and spherical waves (3D), but not for circular waves (2D). Computed results were exact at the limit of stability with Courant number $Cou = 1$. As these are of no practical interest, further tests were done with the maximum Courant number for the 2-dimensional case, i.e., 0.7 (see left graph of Figure 3).

An axisymmetric version of the test code was developed to check the resolution of spherical waves, and the results are pictured to the right-hand side of the same figure. The 56 time steps in these tests correspond to 39 cell-lengths and about 3 wavelengths.

The Improved Numerical Scheme

Although the graphs in Figure 3 seem encouraging the accuracy is actually not sufficient as the error increases with each time step, and after 200 - 300 time steps it becomes unacceptable.

If there are no shocks and the sound field is described by continuous functions, the best way to overcome this difficulty is higher order approximation. Bearing in mind that the final code will be 3-dimensional involving too many neighbours in the numerical scheme does not seem convenient. Based on these arguments a parabolic approximation has been applied to all functions in the finite-volume integrals:

$$\int_{x_0-\frac{h}{2}}^{x_0+\frac{h}{2}} f(x)dx = h[Af(x_0 - h) + (1 - 2A)f(x_0) + Af(x_0 + h)], \; A = \frac{1}{24}.$$

In 2D this means

$$\int_{cell} f(x,y)dxdy = A\sum_{nb} f_{nb} + (1 - 4A)f_{cell},$$

with 'nb' used to denote all four neighbours of a cell in a regular mesh.

The numerical scheme now becomes implicit, so a linear system of equations has to be solved at each time step. Direct methods cannot be considered because of the

Figure 4 Validation of the improved numerical scheme in 1D for *2000* time steps

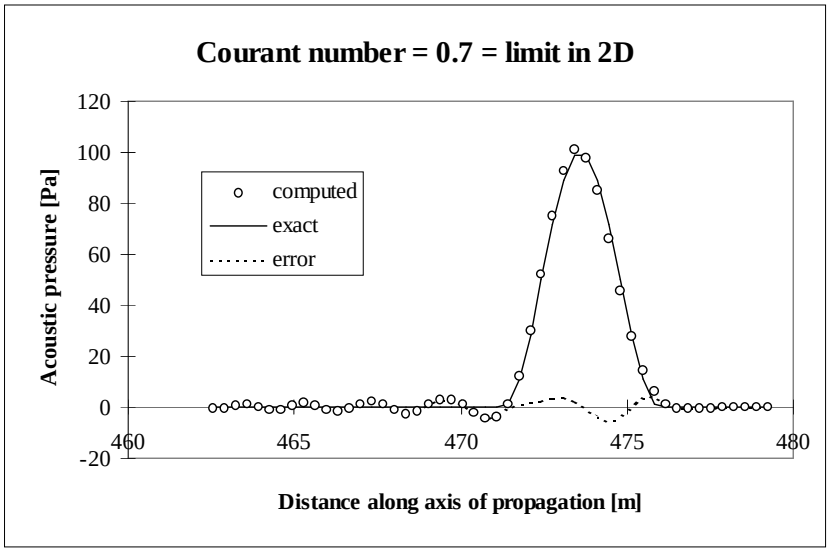

large number of grid points. However, the iterative solution can be provided with a very good initial guess based on the explicit scheme.

When finally the nonlinear terms are implemented in the code their iterations can be done simultaneously with the solution of the linear system.

Tests were performed on the new version in 1D over 2000 time steps. These are equivalent to about 100 wavelengths and seem to be enough to take the signal studied out of the near field. The results shown in Figure 4 exhibit encouraging accuracy. The amplitude of the oscillating numerical error will be about 5% at the boundaries of the near field, which is acceptable. As expected, the efficiency of the algorithm is very high: only 3 to 4 iterations are necessary for convergence at each time step.

4 Coupling of the Subdomains

Since the noise generation domain (near field) is always contained in the propagation domain (far field) all that has to be done is to implement adequate radiating boundary conditions for the near field and to solve it prior to the far field. Time-dependent values of the variables are then imposed on the inner boundaries of the far field, and radiation conditions on its outer boundaries.

With the test version of the code the boundaries have been chosen to be comprised of cell faces (stepwise boundaries). Thus only the time-dependent velocity component that is perpendicular to the boundary has to be determined. This has been done under the assumption that the wave equation holds there (no sources of sound at the boundary), and that the outgoing waves are plane waves. The boundary velocities then can be determined from the velocity field at the previous time step by interpolation. The exact positions of the interpolation points depend on the directions of acoustic

radiation and on the Courant number, and can be calculated for each boundary face.

5 Conclusions and Further Work

A combined decomposition method of both the domain and the variables has been developed that is capable of handling the computationally intensive problems of aeroacoustics.

A solver for the linearized Euler equations has been implemented and tested showing encouraging accuracy. It is a module to be used in both domains for the perturbation variables. Based on a finite-volume staggered grid, the algorithm proposed is stable and efficient.

Future work includes three main stages. First: implementation of the convection terms from (2.3) and (2.4), which have been omitted in this study. (These results will be presented at the 3rd AIAA/CEAS Aeroacoustics Conference in May 1997.) Second: discretization and implementation of the nonlinear terms to complete the acoustic module for the near field. Third: coupling of the acoustic module with a CFD code. In order to build an efficient coupled algorithm, a study has to be done to determine how fine the CFD mesh and time stepping has to be, and whether to include the viscous terms in the acoustic solver.

The combined CFD-CAA code will find environmental applications in studying the mechanisms of generation of aerodynamic noise, and in searching for a way of reducing the noise made by jets, propellers, and wind.

REFERENCES

[Lig52] Lighthill J. M. (1952) On sound generated aerodynamically: I. general theory. In *Proceedings of The Royal Society*, volume 211 A, pages 564–587. London.

[Lyr93] Lyrintzis A. S. (June 1993) The use of kirchhoff's method in computational aeroacoustics. In R.R.Mankbadi, A.S.Lyrintzis, O.Baysal, L.A.Povinelli, and M.Y.Hussaini (eds) *Computational Aero- and Hydro-acoustics*, number 147 in FED, pages 53–61. ASME, New York.

[SH93] Sarkar S. and Hussaini M. (June 1993) A hybrid direct numerical simulation of sound radiated from isotropic turbulence. In R.R.Mankbadi, A.S.Lyrintzis, O.Baysal, L.A.Povinelli, and M.Y.Hussaini (eds) *Computational Aero- and Hydro-acoustics*, number 147 in FED, pages 83–89. ASME, New York.

[SHM95] Shih S., Hixon D., and Mankbadi R. (1995) A zonal approach for prediction of jet noise. *CEAS/AIAA Paper 95-144* .

[VS95] Viswanathan K. and Sankar L. (1995) Numerical simulation of airfoil noise. In A.S.Lyrintzis, R.R.Mankbadi, O.Baysal, and M.Ikegawa (eds) *Computational Aeroacoustics*, number 219 in FED, pages 65–70. ASME, New York.

[ZRL95] Zhang X., Rona A., and Lilley G. (1995) Far-field noise radiation from an unsteady supersonic cavity flow. *CEAS/AIAA Paper 95-040* .